

Manuscript Number: ATMENV-D-14-01926R2

Title: Plume mapping and isotopic characterisation of anthropogenic methane sources

Article Type: Research Paper

Keywords: Plume Mapping, Methane Isotopes, Picarro Mobile

Corresponding Author: Ms. Giulia Zazzeri,

Corresponding Author's Institution: Royal Holloway, University of London

First Author: Giulia Zazzeri

Order of Authors: Giulia Zazzeri; David Lowry; Rebecca E Fisher; James L France; Mathias Lanoisellé; Euan G Nisbet

Abstract: Methane stable isotope analysis, coupled with mole fraction measurement, has been used to link isotopic signature to methane emissions from landfill sites, coal mines and gas leaks in the United Kingdom. A mobile Picarro G2301 CRDS (Cavity Ring-Down Spectroscopy) analyser was installed on a vehicle, together with an anemometer and GPS receiver, to measure atmospheric methane mole fractions and their relative location while driving at speeds up to 80 kph. In targeted areas, when the methane plume was intercepted, air samples were collected in Tedlar bags, for  $\delta^{13}\text{C-CH}_4$  isotopic analysis by CF-GC-IRMS (Continuous Flow Gas Chromatography-Isotopic Ratio Mass Spectroscopy). This method provides high precision isotopic values, determining  $\delta^{13}\text{C-CH}_4$  to  $\pm 0.05$  per mil. The bulk signature of the methane plume into the atmosphere from the whole source area was obtained by Keeling plot analysis, and a  $\delta^{13}\text{C-CH}_4$  signature, with the relative uncertainty, allocated to each methane source investigated. Both landfill and natural gas emissions in SE England have tightly constrained isotopic signatures. The averaged  $\delta^{13}\text{C-CH}_4$  for landfill sites is  $-58 \pm 3$  ‰. The  $\delta^{13}\text{C-CH}_4$  signature for gas leaks is also fairly constant around  $-36 \pm 2$  ‰, a value characteristic of homogenised North Sea supply. In contrast, signatures for coal mines in N. England and Wales fall in a range of  $-51.2 \pm 0.3$  ‰ to  $-30.9 \pm 1.4$  ‰, but can be tightly constrained by region. The study demonstrates that CRDS-based mobile methane measurement coupled with off-line high precision isotopic analysis of plume samples is an efficient way of characterising methane sources. It shows that isotopic measurements allow type identification, and possible location of previously unknown methane sources. In modelling studies this measurement provides an independent constraint to determine the contributions of different sources to the regional methane budget and in the verification of inventory source distribution.

6/03/2015

Dear editor,

Hereby we resubmit our paper "Plume mapping and isotopic characterisation of anthropogenic methane sources" for publication in Atmospheric Environment.

We have appreciated the thoughtful comments of the two reviewers, and we have modified our manuscript to accommodate and answer the questions. In the response to reviewers we indicate point-by-point how we have accommodated their comments.

We hope you will find this revised version acceptable for publication.

With best regards, on behalf of all co-authors,

Giulia Zazzeri

Please address all correspondence to:

Giulia Zazzeri

Giulia.Zazzeri.2011@live.rhul.ac.uk

Phone Number: +447952842253

Yours sincerely,

Giulia Zazzeri, PhD student.

We thank the referees for their positive comments. We have made changes accordingly following their suggests, and we have clarified the points that were raised in the detailed comments below.

**Reviewer #1:**

*L9: 'again' means reader already knows methane trend, I suggest to explain a bit further. Also in the introduction I'd recall the global CH<sub>4</sub> cycle terms, and quantify the relative contribution of landfill, gas leaks and coal mines.*

Thank you for the suggestion. We explained the global CH<sub>4</sub> trend and relative source contributions in a little more depth in the introduction.

*Fig 1: what are the 5x5 big squares? seems resolution is 5 km and only in some areas it has been down-scaled?*

For methane sources like landfills and sewage works the exact location within the site of the emissions are highly uncertain. Therefore, due to this inherent uncertainty, the NAEI methane emissions inventory only resolves the solid and wastewater sectors to 5x5 km, as fixing them to a 1 km<sup>2</sup> grid might be erroneous. However, inventory data are provided at 1km<sup>2</sup> resolution, and this explains why there are those big emission squares, which represent mainly landfill sites.

*L110-113: why not taking natural gas from houses gas taps, instead of going to intersect a plume at far away gas storage facilities? would it work?*

Measuring the isotopic signature of natural gas both from the gas tap in our geochemistry laboratory and in distant storage facilities allowed us to find an isotopic signature that was representative at a regional scale and that could be used in a regional model. Furthermore, the study is a test of how small a plume we can distinguish isotopically by Keeling plot analysis and the reason for multiple transects at further distances downwind of the source.

*L153: did you always have a road perpendicular to the wind direction?*

No, they were not always perpendicular as shown by the Greatness Quarry example, but the wind direction was checked before every measurement campaign and the sampling locations for the day were chosen accordingly, as we needed to be sure that the downwind area of the site was accessible. As we were not measuring fluxes we didn't need the shape of the plume to show a Gaussian distribution.

*L398: [42] is not about airborne measurements.*

Thank you for spotting this. We have changed it.

*Fig. 9 could use same graphics as Fig. 1, also more effective.*

Thanks for the suggestion. We used the original Google Earth output in Figure 9 because it highlights the peaks in methane concentration and it shows that peaks were observed approximately at the same location by driving back and forth for few times along the same downwind transect through the emission plume.

## **Reviewer #2:**

### *Minor Comments*

*1.- Further information on the Picarro parameters, including those related to the operating range (e.g., measuring interval and rise/fall time) should be inserted on page 6, first paragraph.*

Thank you for the suggestion. We inserted more details about Picarro parameters.

*2.- Section 3.1. I have several questions and recommendations:*

*\* Why did the authors select the Mucking and Greatness Quarry landfills for presentation of the results? The reason for this choice should be added.*

It should be pointed out here that some of the sites cannot be covered in more detail because they were measured on site and there is operator and emissions anonymity. Of the remaining sites with public access Mucking and Greatness Quarry are presented in more detail because the samples collected around those locations had the greatest concentration and isotopic range for Keeling plot analysis. Indeed, the two resulting Keeling plots show the best fitting lines and represent very good examples of source signature calculation. We added a sentence to explain that in the revised manuscript. A more detailed paper on landfill methane, including the use of isotopes in understanding methane oxidation, will follow.

*\* The maximum as well as range of methane concentrations measured at each landfill site should be inserted in an additional column of Table 1. Comments on the comparison results found at each landfill site should also be added in this section.*

Thanks for your indication. Concentration ranges were not included since each landfill site was surveyed following a different procedure, depending on observed meteorology, and from

different distances downwind, so as to make the range or maximum concentration recorded meaningless in relation to emissions. Methane concentrations were measured directly on site when the landfill area was accessible (but we have restricted use of the data). In other cases the methane plumes were transected by driving along roads at different distances from the emitting area. If methane emissions from a landfill site are high but are detected far away, methane concentrations recorded are only a few ppb above the background. However, thanks to high precision isotopic measurements, isotopic signatures of source plumes can be determined at near background atmospheric mole fractions. As the aim of this study is the isotopic characterisation of methane areas and not the quantification of emissions, we thought that including concentrations in the table could be misleading.

A proper comparison, including a thorough characterisation of landfill sites, will be provided in a further publication. However, following your suggestion, we have included an explanation for the variability of the results and the range of excess over background recorded by the study.

*\* The text and Figures presented in the paper only refer to the two above landfills mentioned. I strongly believe that, at least, a new column showing the number of samples collected at each landfill should be included in Table I.*

Thanks for the suggestion. We included a new column with the number of Tedlar bag samples collected.

*3.- Section 3.2. I only found the depth of the Thoresby coal mine. Please include the depth of the Aberpergwm and Unity coal mines.*

Thank you for the suggestion. Unfortunately the depth of the Aberpergwm and Unity coal mines could not be retrieved in any documentation available. We will search for that more carefully.

*4.- Page 20, lines 330-333. A reference related to the average values measured in the Lab of the Earth Sciences Department should be included. The same is applicable to the comments written on page 21, lines 360-362.*

The isotopic values that you mention were measured in the RHUL laboratory as part of my PhD study and both averages are the results of tests and samplings that I personally carried out for my thesis work. I still have to submit my thesis and I cannot include a reference for those values. Values from the same gas supply were published by Lowry et al. (2001), but the

isotopic signature of the gas supplied to SE England has changed significantly over the last 15 years and these are not representative of the current supply.

*5.- Page 2, line 51. The reference Lowry et al. (5) written in the manuscript in not number 5 but 28 in the references presented.*

Thank you for spotting this. We have changed it.

# Plume mapping and isotopic characterisation of anthropogenic methane sources

G. Zazzeri<sup>1\*</sup>, D. Lowry<sup>1</sup>, R.E. Fisher<sup>1</sup>, J.L. France<sup>2</sup>, M. Lanoisellé<sup>1</sup> and E.G. Nisbet<sup>1\*</sup>

<sup>1</sup>Royal Holloway, University of London

<sup>2</sup>University of East Anglia

\*Corresponding authors

Giulia Zazzeri

email: [Giulia.Zazzeri.2011@live.rhul.ac.uk](mailto:Giulia.Zazzeri.2011@live.rhul.ac.uk) Phone number: +44 7952 842253

Euan Nisbet

email: [e.nisbet@es.rhul.ac.uk](mailto:e.nisbet@es.rhul.ac.uk) Phone number: +44 1784 443809

## Abstract

Methane stable isotope analysis, coupled with mole fraction measurement, has been used to link isotopic signature to methane emissions from landfill sites, coal mines and gas leaks in the United Kingdom. A mobile Picarro G2301 CRDS (Cavity Ring-Down Spectroscopy) analyser was installed on a vehicle, together with an anemometer and GPS receiver, to measure atmospheric methane mole fractions and their relative location while driving at speeds up to 80 kph. In targeted areas, when the methane plume was intercepted, air samples were collected in Tedlar bags, for  $\delta^{13}\text{C}-\text{CH}_4$  isotopic analysis by CF-GC-IRMS (Continuous Flow Gas Chromatography-Isotopic Ratio Mass Spectroscopy). This method provides high precision isotopic values, determining  $\delta^{13}\text{C}-\text{CH}_4$  to  $\pm 0.05$  per mil.

The bulk signature of the methane plume into the atmosphere from the whole source area was obtained by Keeling plot analysis, and a  $\delta^{13}\text{C}-\text{CH}_4$  signature, with the relative uncertainty, allocated to each methane source investigated. Both landfill and natural gas emissions in SE England have tightly constrained isotopic signatures. The averaged  $\delta^{13}\text{C}-\text{CH}_4$  for landfill sites is  $-58 \pm 3$  ‰. The  $\delta^{13}\text{C}-\text{CH}_4$  signature for gas leaks is also fairly constant around  $-36 \pm 2$  ‰, a value characteristic of homogenised North Sea supply. In contrast, signatures for coal mines in N. England and Wales fall in a range of  $-51.2 \pm 0.3$  ‰ to  $-30.9 \pm 1.4$  ‰, but can be tightly constrained by region.

The study demonstrates that CRDS-based mobile methane measurement coupled with off-line high precision isotopic analysis of plume samples is an efficient way of characterising methane sources. It shows that isotopic measurements allow type identification, and possible location of previously unknown methane sources. In modelling studies this measurement provides an independent constraint to determine the contributions of different sources to the regional methane budget and in the verification of inventory source distribution.

## 1 Introduction

After a steady increase of atmospheric methane in the 1980's and a stabilisation of the global levels between 1999 and 2006, methane concentrations have risen again (Nisbet et al., 2014) with implications for related climate change (Stocker, 2013), but the source contribution to the renewed growth rate is still under debate (Kirschke et al., 2013). Globally, over 60% of total  $\text{CH}_4$  emissions come from human activities, with 22% of emissions from the energy sector and 10% from the waste sector (Dlugokencky et al., 2011). Conurbations such as London emit methane through leaks in the natural gas network, losses from heating systems and other combustion sources, and landfill emissions, which are all highly responsive to achievable control measures. With stricter regulations for landfills and improved maintenance on the gas network, UK national inventories (Webb, 2014) suggest that methane emissions from the waste and natural gas sectors declined throughout the 1990-2012 period. Semi-rural areas around London also contribute. Agriculture is the dominant

43 methane-emitting sector in the UK, accounting for 44 % of total methane emissions in 2012  
44 according to inventories. Emissions from coal mining decreased sharply with the decline of the  
45 industry after 1993 and accounted for only 3 % of all methane emissions in 2012 (Webb, 2014).

46 Methane inventories are compiled from statistical databases (e.g. number of cows, volume of gas  
47 used, etc. multiplied by pre-defined emission factors). This “bottom-up” approach may produce  
48 precise but highly inaccurate estimates, since databases might be incomplete and not updated, and  
49 some emission factors can be poorly established and may differ greatly among countries. Therefore,  
50 although UK national inventories suggest that methane emissions for waste, gas transmission and  
51 coal mining sectors have decreased since 1990 (Webb, 2014), the reduction trend must be verified  
52 by independent measurements. Direct atmospheric (or “top-down”) verification of emission  
53 inventories has been carried out (Lowry et al., 2001).

54 In this study methane stable isotope analyses, coupled with mole fraction measurements, have  
55 been employed to assess proportionate contributions of the main methane sources in SE England.  
56 The source of specific methane emissions can be identified by analysing the methane isotopic  
57 composition, as different source types are characterised clearly by distinct  $^{13}\text{C}$  signatures. Biogenic  
58 methane is  $^{13}\text{C}$  depleted ( $\delta^{13}\text{C} = -50$  to  $-70$  ‰), compared to pyrogenic methane derived from  
59 incomplete combustion ( $\delta^{13}\text{C} = -15$  to  $-30$  ‰) and fossil methane of thermogenic origin ( $\delta^{13}\text{C} \approx -$   
60  $40$  ‰) (e.g. Lasseby et al., 2011). Thus, the proportion of each source category within a source mix  
61 can be estimated and the actual contribution of each methane source in the atmospheric methane  
62 budget constrained. Several studies attest the value of the isotopic analysis as a tool for categorising  
63 methane sources and in verifying inventories (Levin et al., 1999; Lowry et al., 2001; Fisher et al.,  
64 2006; Townsend-Small et al., 2012). For this purpose,  $^{13}\text{C}$  signatures of the methane sources that are  
65 listed in the UK inventories need to be defined accurately.

66 Isotopic data ( $\delta^{13}\text{C}_{\text{CH}_4}$ ) are used in modelling to constrain the contributions of different methane  
67 sources in the mass balance of atmospheric methane at a global and regional scale (Quay et al.,  
68 1991; Mikaloff Fletcher et al., 2004; Bousquet et al., 2006). However, the input values vary from  
69 model to model and the errors on these values are very large at the global scale. Quay et al. (1991)  
70 report a  $\delta^{13}\text{C}_{\text{CH}_4}$  range between  $-46$  and  $-56$  ‰ for landfills. For coal, values of  $-35$  and  $-37$  ‰ are  
71 suggested, whereas the isotopic signature for natural gas is thought to vary from  $-40$  to  $-44$  ‰  
72 (Mikaloff Fletcher et al., 2004; Bousquet et al., 2006; Monteil et al., 2011). Errors can be narrowed  
73 down considerably when the focus is on a regional scale, as this study will prove.

74 This study aims to identify areas of high anthropogenic methane mole fractions in the UK and  
75 link them to specific identifiable sources, using isotopic characterisation. While there have been  
76 many previous studies of  $^{13}\text{C}$  in methane, most are based on small scale processes and few have  
77 been on UK sources (Stahl, 1977; Deines, 1980; Chung et al., 1988; Hitchman et al., 1990;  
78 Bergamaschi et al., 1998; Levin et al., 1999; Whiticar, 1999; Lowry et al., 2001; Klevenhusen et al.,  
79 2010). Lowry et al. (2001) studied isotopic characterisation of specific methane peaks measured  
80 during diurnal air campaigns at the Royal Holloway site, on the western fringe of London, showing  
81 that peaks are derived either from natural gas leaks ( $\delta^{13}\text{C} -33$  ‰ to  $-35$  ‰) or waste treatment  
82 emissions ( $\delta^{13}\text{C} -51$  ‰ to  $-53$  ‰). Nevertheless, the isotopic characteristics of sources may vary



83 over time and season, such as for landfill sites, where the reliance on methane oxidation by topsoil  
84 and gas flaring has been largely replaced by gas extraction systems, and for natural gas because of  
85 different gas source provider countries. Therefore isotopic values need to be regularly reassessed.

86 Sampling campaigns were focused on the targeted sources. A mobile greenhouse gas analyser  
87 (see section 2.3) was installed on board a vehicle to allow measurement of atmospheric methane  
88 mole fractions while driving. A similar setup has been tested already by other studies to measure  
89 methane emissions at large spatial scales (Farrell et al., 2013) and to map methane leaks from a gas  
90 network (Phillips et al., 2013; Eapi et al., 2014). This work validates the use of the instrumentation  
91 for locating methane-emitting areas, as a tool to direct the sample collection for calculating the bulk  
92 isotopic signature of the methane released into the atmosphere.

## 93 **2 Methods**

94 The isotopic composition of methane sources from a 100 m to km-scale spatial area, such as  
95 landfills and open-cut coal mines, needs to be evaluated by assessing integrated emissions from the  
96 whole source site. Measurements of methane mole fractions downwind and upwind of the site  
97 enable a qualitative estimate of the source in terms of its importance in the atmospheric methane  
98 budget. Once the location has been identified as a source of methane emissions, the methane  
99 isotopic analysis of air samples collected downwind across the source plume allows assignment of a  
100 specific  $\delta^{13}\text{C}$  signature to the source in question.

101 Each source investigation required a dedicated sampling campaign. By utilising the mobile gas  
102 analyser, various potential source sites were investigated on the same day, driving on public roads  
103 around the target area and collecting samples whenever relatively high mole fractions were  
104 measured. The mobile gas analyser was also used to detect the locations of gas leaks in a similar  
105 way to Phillips et al. (2013). Methane plumes and spikes are easily measured, and the subsequent  
106 isotopic analysis of the air sampled reveals the origin of these ‘unexpected’ methane peaks of local  
107 origin.

### 108 **2.1 Identification of methane sources**

109 The National Atmospheric Emission Inventory (NAEI) website (<http://naei.defra.gov.uk/>) makes  
110 available total methane emissions per  $\text{km}^2$  per year and is updated annually with some time delay.  
111 Emissions for 2009 for the London region and surrounding boroughs have been mapped using the  
112 ArcGIS software. The resulting emission map (Figure 1), where each square represents one  $\text{km}^2$ ,  
113 offers a picture of the methane emissions distribution in the London area and was used to focus  
114 measurement campaigns. Red squares represent high emission areas. These are sited mainly outside  
115 and on the margins of the London conurbation, whereas central London emissions are uniformly in  
116 the range of 50-100 tonnes /  $\text{km}^2$  / yr. Hotspots were located and identified as first targets for the  
117 measurement campaigns from the map. Their exploration allows the consistency of the emissions  
118 data to be verified and has uncovered many discrepancies.

119 **Figure 1**

## 120 **2.2 Sampling Locations**

121 The 2013 and 2014 monitoring campaigns aimed to characterise isotopically the most important  
122 UK anthropogenic methane sources in terms of tonnes of methane emitted, with a focus on London  
123 conurbation and SE England. Landfills, coal mines and natural gas are the three source categories  
124 that have been assessed in this study (Figure 2). All downwind plumes measured at these sources  
125 were at sub-regulatory levels.

126 **Figure 2**

127 The landfill sites studied are all located within 70 km of London, whereas the evaluation of the  
128 coal mining isotopic signature required an extension of the survey beyond the London area, to  
129 include South Yorkshire, Nottinghamshire, Warwickshire and South Wales. A more detailed study  
130 of the isotopic signatures from UK coal mines is in preparation. The isotopic signature of natural  
131 gas supplied to SE England has been identified by sampling methane plumes downwind of the  
132 British Gas gas storage facility in Staines and downwind of Bacton, on the Norfolk coast, where  
133 pipelines bring all southern and much northern North Sea Norwegian gas onshore, as well as gas  
134 from the interconnector pipeline to Belgium.

## 135 **2.3 Methodology and Material**

### 136 **2.3.1 Picarro Mobile System**

137 The greenhouse gas monitoring system utilised in the monitoring campaigns consists of a mobile  
138 Picarro G2301 CRDS (Cavity Ring-Down Spectroscopy) analyser, which provides a new  
139 measurement of carbon dioxide (CO<sub>2</sub>) and methane (CH<sub>4</sub>) mole fractions in ppm and water vapour  
140 in % every 5 seconds, with a rise and fall time between high and low concentrations that is 90%  
141 accurate in less than 3 seconds. The mobile module (A0941) consists of a pump, control systems for  
142 a Climatronics sonic anemometer and a Hemisphere GPS receiver. Two air inlets, plus the GPS and  
143 sonic anemometer are attached to a mast above the roof of the vehicle at 2.2 m above the ground.  
144 Three fully charged 12 V, 110 Ah lead-acid batteries allow the instrument to run for up to 9 hours.  
145 The airline is ¼" outer diameter and 1.83 m length Nylon tube with the inlet end blocked and a  
146 series of 2mm diameter holes drilled into the first 30 cm to allow ingress of air (air inlet 1 on Figure  
147 3) (Picarro, 2012). This is pumped to the mobile module through a 2 µm Swagelok filter, where the  
148 flow splits allowing approximately 300 cc/min to flow through the Picarro, and the rest of the air to  
149 vent. This greatly reduces the lag time between air entering the inlet and the measurement allowing  
150 successful surveying of small plumes at a vehicle speed of up to 50 km/hr, and large plumes at up to  
151 80 km/hr on first pass. The second air inlet is another ¼" O.D. Nylon tube (air inlet 2 in Figure 3a)  
152 connected to a battery operated diaphragm pump (KNF Neuberger) used to collect plume and  
153 background air samples for later isotopic analysis in the RHUL (Royal Holloway University of  
154 London) laboratory. The pump fills a 5L Tedlar air sample bag in 30 seconds.

155 **Figure 3**

156 The system is controlled by a laptop, so that continuous measurement of CO<sub>2</sub> and CH<sub>4</sub> mole  
157 fractions can be observed by the passenger during travel. Communication between the laptop and

158 the Picarro mobile is by WiFi connection to a 3G or 4G system. Both CH<sub>4</sub> and CO<sub>2</sub> mole fractions  
159 can be displayed in real time on Google Earth, allowing the gas plumes to be geospatially visualised  
160 on site. The time delay between the instantaneous GPS location and the display of Picarro mole  
161 fractions has been calculated as approximately 7 seconds by measuring the time lag of the CO<sub>2</sub> peak  
162 arrival after blowing into the inlet tube.

163 The Picarro 2301 instrument was calibrated in the RHUL greenhouse gas laboratory before each  
164 survey against two National Oceanic and Atmospheric Administration (NOAA) calibrated air  
165 samples, with a resulting precision for CH<sub>4</sub> better than ±0.3 ppb at mole fractions ranging from  
166 1840 and 1975 ppb and accuracies of better than ±1 ppb. A target gas has been analysed using the  
167 Picarro instrument while driving in order to test the stability of measurement during motion, with a  
168 precision of 0.3 ppb (1  $\sigma$ ) over 2 minutes of analysis.

169 The sites of interest were studied by driving downwind and visualising the mole fractions on  
170 Google Earth in real time. At some points plumes could be bisected perpendicular to the wind  
171 direction, allowing the Gaussian shape to be mapped. Changes in wind direction and speed affect  
172 the plume dispersion; methane peaks might also change position and intensity from one pass to the  
173 next downwind of the same methane source. However, the current study is not aimed at calculating  
174 fluxes or accurately pinning down the location of small gas leaks, but at proportioning source inputs  
175 via the isotopic signatures of the sources. A strict accuracy of source position is also not required  
176 for large spatial sources such as landfills and open-cut coal mines where methane plumes can be  
177 easily transected.

178 Once the methane plume was identified, 5L Tedlar bags were filled as close to the plume centre  
179 as possible and at the edges of the plume. When the road traffic conditions allowed, air bags were  
180 collected along the plume transect by stopping the vehicle whenever above-background methane  
181 mole fractions were observed. When sampling was on a major road and the vehicle could not be  
182 stopped, and when the methane mole fraction was not steady during the sampling at a given point  
183 (due to a high variability of the wind direction or obstructions between the source and the road),  
184 samples were collected while driving, at a speed of 48 km/hr (30 mph), giving an integrated sample  
185 over a distance of up to 400 m.

186 **Figure 4**

187 Figure 4 demonstrates an example view of data as seen on Google Earth during sampling. The mole  
188 fraction data were re-plotted during post-analysis using ArcGIS software, utilising satellite images  
189 of the sites as base maps to give a clearer spatial representation of the data.

### 190 2.3.2 Sample Analysis

191 The CH<sub>4</sub> mole fraction data representation along the route provided information on the actual  
192 plume extent, whereas the methane source characteristics were investigated by the isotopic analysis  
193 of the samples collected. CH<sub>4</sub> mole fractions of the air samples in Tedlar bags were measured  
194 independently in the laboratory with a Picarro G1301 CRDS analyser. Each sample was analysed  
195 for 3 minutes, with an average precision of ±0.5 ppb. The carbon isotopic ratio ( $\delta^{13}\text{C}$ ) was measured  
196 in triplicate to high precision (+/- 0.05 ‰) by continuous flow gas chromatography isotope ratio

197 mass spectrometry (CF GC-IRMS) (Fisher et al., 2006). This ratio is expressed in  $\delta$  notation from  
198 the following equation:

$$199 \quad \delta = (R_A/R_{std} - 1) \times 1000$$

200 (Eq 1)

201 where  $R_A$  denotes the isotopic ratio in  $\text{CO}_2$  derived by combustion of the methane sample  
202 ( $^{13}\text{C}/^{12}\text{C}$ ) and  $R_{std}$  is the corresponding ratio in the  $\text{CO}_2$  reference gas which is calibrated to the V-  
203 PDB scale for  $\delta^{13}\text{C}$  using international standards. The isotopic ratio is expressed as per mil (‰).

### 204 2.3.3 Keeling Plot approach

205 The signature of each methane source (or mixture of sources in an urban conurbation) was  
206 characterised using the Keeling plot method (Keeling, 1958). According to this approach,  $\delta^{13}\text{C}$   
207 values must be plotted against the inverse of mole fraction data to calculate the isotopic signature of  
208 the methane source responsible for the excess over background. Following the Keeling plot  
209 procedure, one isotopic signature (with calculated error to allow for some variability of source  
210 methane production pathways) was assigned to every methane source explored.

#### 211 Keeling Plot and the regression analysis

212 The atmospheric mixing ratio (mole fraction) of a gas ( $c_a$ ) in the lower boundary layer results  
213 from the combination of the background atmospheric mole fraction ( $c_b$ ) and the mole fraction of the  
214 gas added by the source ( $c_s$ ) (Pataki et al., 2003):

$$215 \quad c_a = c_b + c_s$$

216 (Eq 2)

217 By assuming the conservation of mass, the  $\delta^{13}\text{C}$  signature of the source input to atmosphere can  
218 be calculated as follows:

$$219 \quad \delta^{13}C_a = c_b (\delta^{13}C_b - \delta^{13}C_s) \cdot 1/c_a + \delta^{13}C_s$$

220 (Eq 3)

221  $\delta^{13}C_a$  and  $1/c_a$  values are respectively the y and the x values of a best-fit line, whose intercept (at  
222  $1/c_a = 0$ ) is the isotopic value at which the methane mole fraction tends to infinity. This is  
223 interpreted as the isotope signature of the methane source responsible for the excess over  
224 background.

225 A linear regression of data must be performed in order to compute the line slope and intercept.  
226 However, the estimate of the line parameters might be biased if an ordinary least squared (OLS)  
227 method is applied (as in many spreadsheets), which assumes errors are confined to the dependent  
228 variable (Leng et al., 2007). For our sources, both variables are measured with errors and another  
229 regression model must be implemented. Moreover, our measurements are affected by  
230 heteroscedasticity, where the error of a variable changes across the range of values of a second  
231 variable that predicts it (Berry and Feldman, 1985). Errors may increase as the value of the  
232 independent variable ( $1/[\text{CH}_4]$ ) is decreasing, as higher mole fractions are measured with higher  
233 standard deviations. Although there are several fitting models that allow for errors in the  
234 independent variable (Sokal and Rohlf, 1995), e.g. orthogonal distance regression and geometric  
235 mean regression (recommended by Pataki (2003)), few models accommodate for heteroscedastic

236 measurement errors. If a typical OLS approach, intended to minimize  $\sum e_i^2$ , is applied in case of  
237 heteroscedasticity, the calculation of the regression line would give greater emphasis to the extreme  
238 values (with greater errors), which are conversely less precise and, hence, contain less information.

239 Akritas et al. (1996) introduced the BCES estimators procedure (for Bivariate Correlated Errors  
240 and intrinsic Scatter). This statistical procedure, designed to overcome the heteroscedasticity case,  
241 accounts for correlated errors between the two variables and allows for the magnitude of  
242 measurement errors to be dependent on the measurements. These features make the BCES approach  
243 well suited for computing the slope and the intercept of the Keeling plot. Therefore the BCES  
244 regression program, available to download  
245 (<http://www.astro.wisc.edu/~mab/archive/stats/stats.html>), has been used to find the Keeling plot  
246 intercept with the relative uncertainty, and so the  $\delta^{13}\text{C}$  value of the methane source. This technique  
247 results in a much more robust calculation of source signature but will only give very tightly  
248 constrained ‰ errors when the precision of both mole fraction and isotopic measurements are very  
249 high and the  $\delta^{13}\text{C}$  of the source signature is homogenous across the plume (i.e. single source).

## 250 **3 Results**

### 251 **3.1 Landfill sites**

252 The widest plumes and highest recorded mole fractions of methane were from landfill sites, both  
253 still active and recently closed, as suggested by the UK national inventories. The excess methane  
254 over background recorded off site ranged from 0.1 ppm to 15 ppm.

#### 255 **Table 1**

256 Isotopic signatures observed for all the landfill studied (Table 1) span a range from  $-60.2 \pm 1.4$  to  
257  $-55.2 \pm 0.6$  ‰, with an averaged value of  $-58.0 \pm 3$  (2SD) ‰. Wapsey's Wood was surveyed twice,  
258 in July and April, and the identified isotopic signature was consistent. The isotopic variability  
259 among sites depends upon several parameters such as waste composition, temperature and the level  
260 of methane oxidation performed by methanotrophic bacteria in the top-soil cover (Liptay et al.,  
261 1998).

262 The two landfill sites presented herein, Mucking and Greatness Quarry, were carefully surveyed  
263 thanks to the accessibility of public roads downwind of the sites, obtaining a wide range of mole  
264 fraction values for Keeling plot analysis.

265 Although it was closed in 2012, Mucking landfill (Figure 5a) is still emitting a large amount of  
266 methane: the maximum mole fraction recorded in the measured part of the plume was  
267 approximately 17 ppm. With wind from the SSW it was possible to intersect the plume on 4  
268 transects at different distances from the NNE side of the landfill and 11 samples were collected,  
269 covering a wide range of mole fractions, ideal for precise Keeling plot analysis.

270 The intercept of the Keeling plot based on all the samples collected in the vicinity of the landfill  
271 is  $-56.1 \pm 0.5$ ‰ (2SD) (Figure 6a).

272 Greatness Quarry (Figure 5b) is an active landfill site to the north of the town of Sevenoaks,  
273 which was surveyed on the 24<sup>th</sup> of October 2013. A methane plume was intercepted along the NW

274 side of the landfill and 8 samples were collected for isotopic analysis. An averaged isotopic  
275 signature for the plume of  $-57.4 \pm 0.5$  ‰ (2SD) resulted from Keeling plot analysis of samples  
276 (Figure 6b).

277 **Figure 5**

278 **Figure 6**

279 These two landfill sites, taken as representative examples of UK landfills, show a similar  
280 isotopic signature, although Mucking landfill was closed in 2012, while the Greatness Quarry is still  
281 active.

## 282 **3.2 Coal Mines**

283 **Table 2**

284 Thoresby colliery in Nottinghamshire is one of the deep mines investigated for this study. It is  
285 one of the UK's largest coal mines but scheduled for closure in 2015. Mining is currently taking  
286 place at about 650 m underground. Although methane is drained off for 2.8 MWe electrical power  
287 generation (Holloway et al., 2005), mole fraction levels up to 4.6 ppm were observed in the  
288 downwind plume. As Figure 7a shows, the methane plume was transected three times and 9  
289 samples were collected. The resulting Keeling plot intercept is  $-51.2 \pm 0.3$  ‰ (2SD).

290 Aberpergwm and Unity deep coal mines in Wales (Figure 7b), which closed in December 2012  
291 and in October 2013 respectively, were investigated on 17<sup>th</sup> October 2013. Mole fraction peaks of 6  
292 ppm were observed downwind of both deep mines. The Keeling plots based on the samples  
293 collected near these deep mines give an isotopic source signature of  $-33.3 \pm 1.8$  ‰ for Aberpergwm  
294 and  $-30.9 \pm 1.4$  ‰ for the Unity colliery, both highly <sup>13</sup>C-enriched relative to Thoresby colliery  
295 (Figure 8).

296 **Figure 7**

297 **Figure 8**

298 The coal exploited in Thoresby colliery, as in all deep English coal mines, is bituminous coal (Hill,  
299 2001), whereas collieries in the north-west coalfield area of Wales exploit pure anthracite (Alderton  
300 et al., 2004). The characterisation of methane released from different coal types suggests a link  
301 between enrichment in the <sup>13</sup>C content of methane emitted to atmosphere with progression of coal  
302 rank as previously alluded to by Chung and Sackett (1979). This hypothesis will be tested by further  
303 study of coalfield composition for comparison with plumes sampled at other UK coal mines.

## 304 **3.3 Natural Gas signature**

305 **Table 3**

Staines and Bacton (Figure 2 for the location) have been chosen as sampling sites for assessing the  
isotopic signature of natural gas. A 1.2 km path was surveyed on the south (downwind side) of the  
Staines storage facility and 16 samples were collected for isotopic analysis with mole fractions  
ranging from 1.98 to 3.85 ppm. The Keeling plot for the whole transect (Figure 11a) shows a  
constant origin for the methane of  $-36.3 \pm 0.3$  ‰ that is consistent with a dominantly thermogenic  
North Sea gas source (Lowry et al., 2001). It suggests that there are other leaks in the gas

distribution system along with the storage tank (“gasometer”) that is located in the middle of the transect (Figure 9).

306 **Figure 9**

307 Mole fractions up to 24 ppm were recorded in the plume downwind of Bacton and 19 air samples  
308 were collected for isotopic analysis. An isotopic signature of  $-35.7 \pm 1.2$  ‰ was observed (Figure  
309 11b), which is consistent with the isotopic value that has been ascribed to Staines gas works.

310 **Figure 10**

311 **Figure 11**

312 The intercept values of  $-36.3 \pm 0.3$  ‰ and  $-35.7 \pm 1.2$  ‰ are both in good agreement with the  
313 averaged value of  $-37.3 \pm 0.9$  ‰ (2SD) obtained by collecting monthly samples of natural gas in the  
314 geochemistry lab of the Earth Sciences Department at RHUL and measuring their isotopic  
315 signatures.

## 316 **4 Discussion and Conclusions**

317 This study focuses on the isotopic characterisation of methane emission plumes from major UK  
318 anthropogenic methane sources. Landfill sites, coal mines and gas leaks have been surveyed and  
319 sampled using a mobile system based around the Picarro G2301 instrument. A  $\delta^{13}\text{C}$  signature has  
320 been allocated to each methane source that has been investigated by the isotopic analysis of samples  
321 collected at each site. The  $\delta^{13}\text{C}$  signatures for landfill sites span a range between  $-60.2 \pm 1.4$  ‰  
322 (2SD) and  $-55.2 \pm 0.6$  ‰ (2SD), whereas signatures for coal mines fall within a range of  $-51.2 \pm$   
323  $0.3$  ‰ (2SD) to  $-30.9 \pm 1.4$  ‰ (2SD). The  $^{13}\text{C}$  signature for gas leaks is found to be fairly constant  
324 around  $-36 \pm 2$  ‰ (2SD).

325 Detailed exploration of an area the size of a landfill or open-cut coal mine in its entire extent,  
326 measuring gas mole fractions, fluxes and isotopic signatures in order to estimate its contribution in  
327 terms of methane emissions, requires time consuming and labour-intensive procedures (e.g. flux  
328 chamber technique). Several previous studies have investigated isotopic signatures of methane  
329 emissions from landfills using flux chambers to capture methane fluxes from the soil and collect air  
330 samples (Liptay et al., 1998; Chanton and Liptay, 2000). In order to ensure a representative area is  
331 covered, many chambers need to be arranged across the site, often highlighting the large spatial  
332 variability of the  $^{13}\text{C}$  signature measured. Isotopic signatures of landfill emissions from covered  
333 areas have been shown to differ from uncapped active tipping areas, due to the oxidation mediated  
334 by methanotrophic bacteria in the cover soil (Bergamaschi et al., 1998). Bergamaschi et al. (1998)  
335 obtained values highly enriched ( $-45.9 \pm 8$  ‰) in covered areas relative to those observed in  
336 uncovered areas ( $-55.1 \pm 5.2$  ‰).

337 When the methane plume downwind of a landfill is intercepted and analysed, the overall  
338 signature of the methane released into the atmosphere from the whole site can be estimated, which  
339 is the number needed at a minimum of regional level for atmospheric inversion models. The  
340 isotopic signatures of methane emissions from SE England landfills do not show great variability  
341 and a value of  $-58$  ‰ could be safely used as model input for the whole of UK  $\text{CH}_4$  emissions from

342 active or recently closed landfills. Emissions from old landfills that predate gas extraction will  
343 likely account for a small proportion of emissions that are more enriched in  $\delta^{13}\text{C}$  toward -50 ‰. As  
344 methane emissions from landfills can isotopically change over time, following enhanced landfill  
345 management schemes (e.g. gas extraction), systematic measurements of  $^{13}\text{C}$  signatures of methane  
346 emissions need to be carried out in order to provide up-to-date and more representative values.

347 The isotopic range for coal is found to be relatively wide, compared to those assigned to landfill  
348 and natural gas emissions. Many factors are involved and might explain the variety of isotopic  
349 values measured, such as the depth of coal seams and coal rank. Preliminary results suggest a  $^{13}\text{C}$   
350 enrichment of methane with progression of rank, which needs to be confirmed with further  
351 sampling campaigns with the Picarro mobile system around other UK coal mines.

352 The  $\delta^{13}\text{C}$  range for the natural gas source has been constrained to a value of -36 ‰, which  
353 represents the isotopic signature of the natural gas supplied to the whole of SE England. Natural gas  
354 samples from Holland and Italy were analysed at RHUL, giving values of  $-29.5 \pm 0.09$  ‰ (2SD)  
355 and  $-46.7 \pm 0.09$  ‰ (2SD) respectively. In the NW European Atlas report (Lokhorst, 1997), carbon  
356 isotope ratios between -33 and -36 ‰ for the Carboniferous reservoir gas in the North Sea and  
357 between -30 and -24 ‰ for the Rotliegend strata in the southern North Sea are indicated. The  
358 natural gas supply from western Siberia has been measured near source, and in St. Petersburg by the  
359 RHUL group and in Heidelberg by Levin et al. (1999) and is characterised by an isotopic signature  
360 of approximately -50 ‰. The isotopic value of the natural gas supply to SW London has changed  
361 little in recent years, being close to -34‰ over the 1998-99 period (Lowry et al., 2001) and close to  
362 -36‰ since at least 2002, and the new data show that this figure can be applied to emissions from a  
363 much larger region of England.

364 By using the Picarro mobile system, the survey of methane sources can be focused on a specific  
365 region or country, obtaining more precise isotopic values to be used in regional models.  
366 Furthermore, the isotopic precision of  $\pm 0.05$  ‰ achieved by CF GC-IRMS on collected samples  
367 is significantly better than current laser-based isotopic measurement systems, such as the CRDS  
368 analyser, which is within 1 ‰ for  $\delta^{13}\text{C}$  of  $\text{CH}_4$  (Phillips et al., 2013) operating under similar  
369 conditions of mobile measurement. This means that precise isotopic signatures of source plumes  
370 can be determined at near background atmospheric mole fractions (50 ppb excess  $\text{CH}_4$  for a 20 ‰  
371 difference between source and background air isotopic signatures, 100 ppb for 10 ‰ difference, 200  
372 ppb for 5 ‰).

373 In areas with multiple sources, such as urban conurbations, where leaks in the natural gas supply  
374 pipes can occur near landfill sites and sewage works, high precision isotopic measurements allow  
375 different potential sources to be carefully distinguished. Due to the mixed nature of methane  
376 sources and their temporal variability, the evaluation of methane fluxes in urban environments  
377 involves numerous observations and measurement techniques, including the eddy covariance  
378 method (Gioli et al., 2012), techniques based on a mass balance approach (Zimnoch et al., 2010)  
379 and airborne measurements allowing a large surface footprint (O'shea et al., 2014). The estimated  
380 methane fluxes are then linked to methane sources using inventory data. The high uncertainty



381 affecting inventories is therefore propagated to the source partitioning, whereas isotopic  
382 measurements provide an independent constraint on source proportions.

383 To conclude, the Picarro mobile methane measurement system, coupled with the isotope analysis  
384 of sampled methane emissions by high precision CF GC-IRMS, is an efficient way of locating and  
385 precisely identifying methane emissions by source, since it enables a large spatial coverage and  
386 rapid location of downwind plumes in the survey of methane source areas. The instantaneous  
387 display of methane mole fractions during the survey allows the methane plume extent to be directly  
388 visualized and sample collection to be carefully directed. The technique can be further applied to  
389 detect small leaks from gas pipelines and fugitive emissions from alternative methane sources.  
390 Therefore this system can be widely employed and has the potential to help in the reduction of  
391 methane emissions in a cost effective manner.

### 392 **Acknowledgements**

393 Giulia Zazzeri would like to thank Royal Holloway, University of London for provision of a  
394 Crossland scholarship and a contribution from the Department of Earth Sciences from 2011 to  
395 2014. Thanks to WRG (now FCC environment) for access into 2 of the landfill sites included in this  
396 study, Chris Rella of Picarro Inc. for discussion of the mobile module measurement technique and  
397 Picarro Support for fault-finding.

398

- 400 <http://naei.defra.gov.uk/>.
- 401 <http://www.astro.wisc.edu/~mab/archive/stats/stats.html>.
- 402 Akritas, M.G., and Bershad, M.A., 1996, Linear regression for astronomical data with  
403 measurement errors and intrinsic scatter: *Astrophysical Journal*, v. 470, p. 706-714.
- 404 Alderton, D., Oxtoby, N., Brice, H., Grassineau, N., and Bevins, R., 2004, The link between fluids  
405 and rank variation in the South Wales Coalfield: evidence from fluid inclusions and stable  
406 isotopes: *Geofluids*, v. 4, p. 221-236.
- 407 Bergamaschi, P., Lubina, C., Königstedt, R., Fischer, H., Veltkamp, A., and Zwaagstra, O., 1998,  
408 Stable isotopic signatures ( $\delta^{13}\text{C}$ ,  $\delta\text{D}$ ) of methane from European landfill sites: *Journal of*  
409 *Geophysical Research: Atmospheres* (1984–2012), v. 103, p. 8251-8265.
- 410 Berry, W.D., and Feldman, S., 1985, *Multiple regression in practice*, Sage.
- 411 Bousquet, P., Ciais, P., Miller, J., Dlugokencky, E., Hauglustaine, D., Prigent, C., Van der Werf, G.,  
412 Peylin, P., Brunke, E.-G., and Carouge, C., 2006, Contribution of anthropogenic and natural  
413 sources to atmospheric methane variability: *Nature*, v. 443, p. 439-443.
- 414 Chanton, J., and Liptay, K., 2000, Seasonal variation in methane oxidation in a landfill cover soil as  
415 determined by an in situ stable isotope technique: *Global Biogeochemical Cycles*, v. 14, p.  
416 51-60.
- 417 Chung, H.M., Gormly, J., and Squires, R., 1988, Origin of gaseous hydrocarbons in subsurface  
418 environments: theoretical considerations of carbon isotope distribution: *Chemical Geology*,  
419 v. 71, p. 97-104.
- 420 Chung, H.M., and Sackett, W.M., 1979, Use of stable carbon isotope compositions of pyrolytically  
421 derived methane as maturity indices for carbonaceous materials: *Geochimica et*  
422 *Cosmochimica Acta*, v. 43.
- 423 Deines, P., 1980, The isotopic composition of reduced organic carbon: *Handbook of environmental*  
424 *isotope geochemistry*, p. 329-406.
- 425 Dlugokencky, E.J., Nisbet, E.G., Fisher, R., and Lowry, D., 2011, Global atmospheric methane:  
426 budget, changes and dangers: *Philosophical Transactions of the Royal Society A:*  
427 *Mathematical, Physical and Engineering Sciences*, v. 369, p. 2058-2072.
- 428 Eapi, G.R., Sabnis, M.S., and Sattler, M.L., 2014, Mobile Measurement of Methane and Hydrogen  
429 Sulfide at Natural Gas Production Site Fence Lines in the Texas Barnett Shale: *Journal of*  
430 *the Air & Waste Management Association*.
- 431 Farrell, P., Culling, D., and Leifer, I., 2013, Transcontinental methane measurements: Part 1. A  
432 mobile surface platform for source investigations: *Atmospheric Environment*, v. 74, p. 422-  
433 431.
- 434 Fisher, R., Lowry, D., Wilkin, O., Sriskantharajah, S., and Nisbet, E.G., 2006, High-precision,  
435 automated stable isotope analysis of atmospheric methane and carbon dioxide using  
436 continuous-flow isotope-ratio mass spectrometry: *Rapid Communications in Mass*  
437 *Spectrometry*, v. 20, p. 200-208.
- 438 Gioli, B., Toscano, P., Lugato, E., Matese, A., Miglietta, F., Zaldei, A., and Vaccari, F., 2012,  
439 Methane and carbon dioxide fluxes and source partitioning in urban areas: The case study of  
440 Florence, Italy: *Environmental pollution*, v. 164, p. 125-131.
- 441 Hill, A., 2001, *The South Yorkshire Coalfield: A History and Development*.
- 442 Hitchman, S., Darling, W., and Williams, G., 1990, Stable isotope ratios in methane containing  
443 gases in the United Kingdom.
- 444 Holloway, S., Jones, N., Creedy, D., and Garner, K., 2005, Can new technologies be used to exploit  
445 the coal resources in the Yorkshire-Nottinghamshire coalfield?
- 446 Keeling, C.D., 1958, The concentration and isotopic abundances of atmospheric carbon dioxide in  
447 rural areas: *Geochimica et Cosmochimica Acta*, v. 13, p. 322-334.
- 448 Kirschke, S., Bousquet, P., Ciais, P., Saunoy, M., Canadell, J.G., Dlugokencky, E.J., Bergamaschi,  
449 P., Bergmann, D., Blake, D.R., and Bruhwiler, L., 2013, Three decades of global methane  
450 sources and sinks: *Nature Geoscience*, v. 6, p. 813-823.

- 451 Klevenhusen, F., Bernasconi, S.M., Kreuzer, M., and Soliva, C.R., 2010, Experimental validation of  
452 the Intergovernmental Panel on Climate Change default values for ruminant-derived  
453 methane and its carbon-isotope signature: *Animal Production Science*, v. 50, p. 159-167.
- 454 Lassey, K.R., Allan, W., and Fletcher, S.E.M., 2011, Seasonal inter-relationships in atmospheric  
455 methane and companion delta C-13 values: effects of sinks and sources: *Tellus Series B-*  
456 *Chemical and Physical Meteorology*, v. 63, p. 287-301.
- 457 Leng, L., Zhang, T., Kleinman, L., and Zhu, W., 2007, Ordinary least square regression, orthogonal  
458 regression, geometric mean regression and their applications in aerosol science, *Journal of*  
459 *Physics: Conference Series*, Volume 78, IOP Publishing, p. 012084.
- 460 Levin, I., Glatzel-Mattheier, H., Marik, T., Cuntz, M., Schmidt, M., and Worthy, D.E., 1999,  
461 Verification of German methane emission inventories and their recent changes based on  
462 atmospheric observations: *Journal of Geophysical Research: Atmospheres (1984–2012)*, v.  
463 104, p. 3447-3456.
- 464 Liptay, K., Chanton, J., Czepiel, P., and Mosher, B., 1998, Use of stable isotopes to determine  
465 methane oxidation in landfill cover soils: *Journal of Geophysical Research: Atmospheres*  
466 *(1984–2012)*, v. 103, p. 8243-8250.
- 467 Lokhorst, A., 1997, NW European Gas Atlas, British Geological Survey (BGS), Bundesanstalt für  
468 Geowissenschaften und Rohstoffe (BGR), Danmarks og Grønlands Geologiske  
469 Undersøgelse (GEUS), Panstwowy Instytut Geologiczny (PGI), Nederlands Instituut voor  
470 Toegepaste Geowetenschappen TNO (NITG-TNO), European Union.
- 471 Lowry, D., Holmes, C.W., Rata, N.D., O'Brien, P., and Nisbet, E.G., 2001, London methane  
472 emissions: Use of diurnal changes in concentration and  $\delta^{13}\text{C}$  to identify urban sources and  
473 verify inventories: *Journal of Geophysical Research: Atmospheres*, v. 106, p. 7427-7448.
- 474 Mikaloff Fletcher, S.E., Tans, P.P., Bruhwiler, L.M., Miller, J.B., and Heimann, M., 2004, CH<sub>4</sub>  
475 sources estimated from atmospheric observations of CH<sub>4</sub> and its <sup>13</sup>C/<sup>12</sup>C isotopic ratios: 2.  
476 Inverse modeling of CH<sub>4</sub> fluxes from geographical regions: *Global Biogeochemical Cycles*,  
477 v. 18.
- 478 Monteil, G., Houweling, S., Dlugokenky, E., Maenhout, G., Vaughn, B., White, J., and Rockmann,  
479 T., 2011, Interpreting methane variations in the past two decades using measurements of  
480 CH<sub>4</sub> mixing ratio and isotopic composition: *Atmospheric chemistry and physics*, v. 11, p.  
481 9141-9153.
- 482 Nisbet, E.G., Dlugokenky, E.J., and Bousquet, P., 2014, Methane on the rise—again: *Science*, v.  
483 343, p. 493-495.
- 484 O'Shea, S.J., Allen, G., Fleming, Z.L., Bauguitte, S.J.B., Percival, C.J., Gallagher, M.W., Lee, J.,  
485 Helfter, C., and Nemitz, E., 2014, Area fluxes of carbon dioxide, methane, and carbon  
486 monoxide derived from airborne measurements around Greater London: A case study during  
487 summer 2012: *Journal of Geophysical Research: Atmospheres*, v. 119, p. 4940-4952.
- 488 Pataki, D.E., Bowling, D.R., and Ehleringer, J.R., 2003, Seasonal cycle of carbon dioxide and its  
489 isotopic composition in an urban atmosphere: Anthropogenic and biogenic effects: *Journal*  
490 *of Geophysical Research-Atmospheres*, v. 108.
- 491 Phillips, N.G., Ackley, R., Crosson, E.R., Down, A., Hutyra, L.R., Brondfield, M., Karr, J.D., Zhao,  
492 K., and Jackson, R.B., 2013, Mapping urban pipeline leaks: Methane leaks across Boston:  
493 *Environmental pollution*, v. 173, p. 1-4.
- 494 Picarro, 2012, Picarro Mobile Kit User's Guide 40047 Revision B.
- 495 Quay, P., King, S., Stutsman, J., Wilbur, D., Steele, L., Fung, I., Gammon, R., Brown, T., Farwell,  
496 G., and Grootes, P., 1991, Carbon isotopic composition of atmospheric CH<sub>4</sub>: Fossil and  
497 biomass burning source strengths: *Global Biogeochemical Cycles*, v. 5, p. 25-47.
- 498 Sokal, R.R., and Rohlf, F.J., 1995, *Biometry: the principals and practice of statistics in biological*  
499 *research*: WH Freeman and Company, New York.
- 500 Stahl, W.J., 1977, Carbon and nitrogen isotopes in hydrocarbon research and exploration: *Chemical*  
501 *Geology*, v. 20, p. 121-149.

- 502 Stocker, D.Q., 2013, Climate change 2013: The physical science basis: Working Group I  
 503 Contribution to the Fifth Assessment Report of the Intergovernmental Panel on Climate  
 504 Change, Summary for Policymakers, IPCC.  
 505 Townsend-Small, A., Tyler, S.C., Pataki, D.E., Xu, X.M., and Christensen, L.E., 2012, Isotopic  
 506 measurements of atmospheric methane in Los Angeles, California, USA: Influence of  
 507 "fugitive" fossil fuel emissions: *Journal of Geophysical Research-Atmospheres*, v. 117.  
 508 Webb, B.M., Brown P, Buys G, Cardenas L, Murrells T, Pang Y, Passant N, Thistlethwaite G,  
 509 Watterson J 2014, UK Greenhouse Gas Inventory, 1990 to 2012.  
 510 Whiticar, M.J., 1999, Carbon and hydrogen isotope systematics of bacterial formation and oxidation  
 511 of methane: *Chemical Geology*, v. 161, p. 291-314.  
 512 Zimnoch, M., Godłowska, J., Necki, J., and Rozanski, K., 2010, Assessing surface fluxes of CO<sub>2</sub>  
 513 and CH<sub>4</sub> in urban environment: a reconnaissance study in Krakow, Southern Poland: *Tellus*  
 514 B, v. 62, p. 573-580.  
 515

## 516 List of captions

517 **Figure 1** London Region emission map derived from 1 km<sup>2</sup> methane emission data for 2009 from the NAEI website . Red  
 518 squares represent high emission areas. These are sited mainly outside and on the margins of the London conurbation,  
 519 whereas central London emissions are uniformly in the range of 50-100 tonnes / km<sup>2</sup> / yr.

520 **Figure 2** Map of the sites surveyed for this study. White diamonds represent the landfill sites studied. Black diamonds  
 521 indicate Bacton, on the Norfolk coast, and the gas storage facility in Staines, on the west side of London region. White  
 522 pentagons represent coal mines.

523 **Figure 3** a) Schematic set up of the RHUL Picarro mobile measurement system and all the physical connections b)  
 524 Picarro Mobile c) vehicle used in the sampling campaigns.

525 **Figure 4** Google Earth view of methane plumes detected around Mucking landfill location on 14<sup>th</sup> October 2013. The  
 526 maximum mole fractions are labelled for each source plume measured.

527 **Figure 5** ArcGIS plot of methane mole fractions in ppm recorded on 14<sup>th</sup> October 2013 around Mucking landfill site (a)  
 528 and on 24<sup>th</sup> October 2013 around Greatness Quarry landfill site (b). The grid coordinates are displayed in the British  
 529 National Coordinate System. The red arrow represents the wind direction.

530 **Figure 6** Keeling plot based on the samples collected around Mucking landfill site (a) and around Greatness Quarry  
 531 landfill site (b). Error bars are not shown as they are smaller than displayed symbols.

532 **Figure 7** ArcGIS plot of methane mole fractions in ppm recorded on 22<sup>nd</sup> November 2013 around Thoresby Colliery (a)  
 533 and on 17<sup>th</sup> October 2013 around Aberpergwm and Unity deep mines in Wales (b). The grid coordinates are displayed in the  
 534 British National Coordinate System. The red arrow represents the wind direction. Stars represent the coal mine locations.

535 **Figure 8** Keeling plots based on samples collected downwind of two deep mines in Wales (Aberpergwm and Unity coal  
 536 mines) on 17<sup>th</sup> October 2013 and the Thoresby Colliery on 22<sup>nd</sup> November 2013. Error bars are not shown as they are smaller  
 537 than displayed symbols.

538 **Figure 9** Sample locations (yellow markers) and mole fraction peaks measured downwind of gas works in Staines (3 km  
 539 ENE of RHUL) on 11<sup>th</sup> April 2014. 16 samples were collected for isotopic analysis, with mole fractions ranging from 1.98 to  
 540 3.85 ppm.

541 **Figure 10** ArcGIS plot of methane mole fractions in ppm recorded on 30<sup>th</sup> of April 2014 around Bacton gas terminals.  
 542 The grid coordinates are displayed in the British National Coordinate System. The red arrow represents the wind direction.

543 **Figure 11** Keeling plot based on samples collected downwind of gas works in Staines on 11<sup>th</sup> April 2014 (a) and downwind  
 544 of gas terminals in Bacton on 30<sup>th</sup> April 2014 (b). Error bars are not shown as they are smaller than displayed symbols.

545 **Table 1** Landfill surveyed with the calculated  $\delta^{13}\text{C}$  signature. Errors are calculated as 2 standard deviations. An averaged  
 546 value of  $-58.0 \pm 3$  (2SD) ‰ was calculated.

547 **Table 2** Collieries discussed in the text and  $\delta^{13}\text{C}$  signatures of methane plumes sampled. Errors in the  $^{13}\text{C}$  signature are  
 548 calculated as 2 standard deviations.

549 **Table 3** Gas installations discussed in the text and  $\delta^{13}\text{C}$  signatures of methane plumes sampled. Errors in the  $^{13}\text{C}$   
 550 signature are calculated as 2 standard deviations.

551

552 **List of figures**

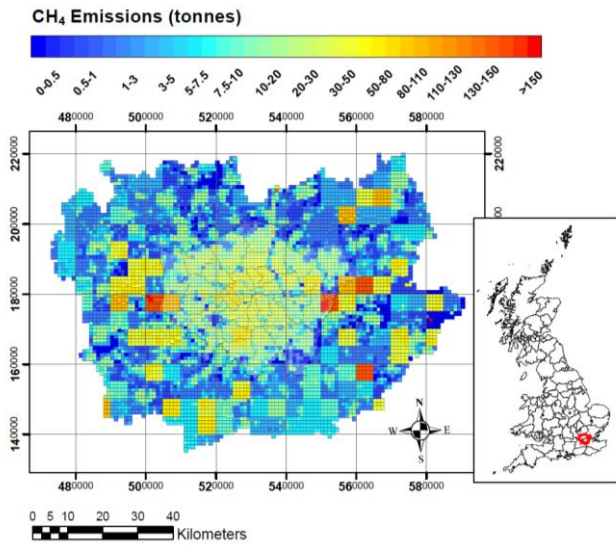


**Figure 1**

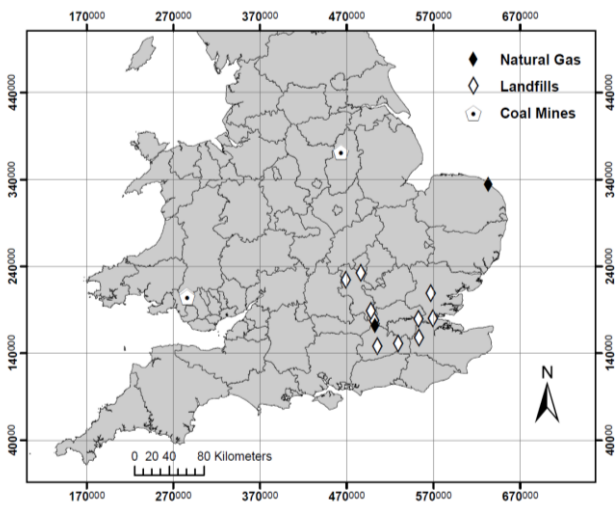


**Figure 2**

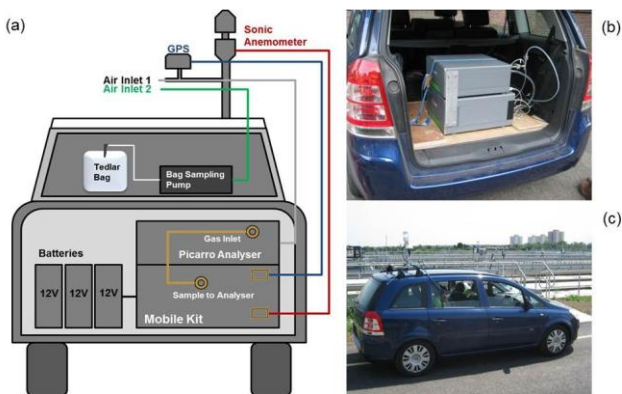


**Figure 3**

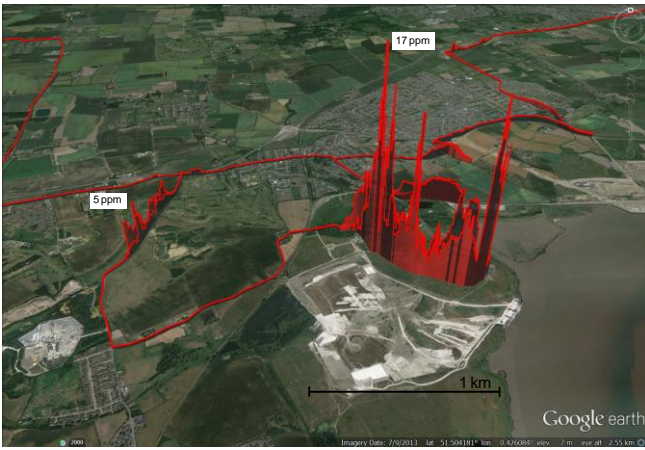
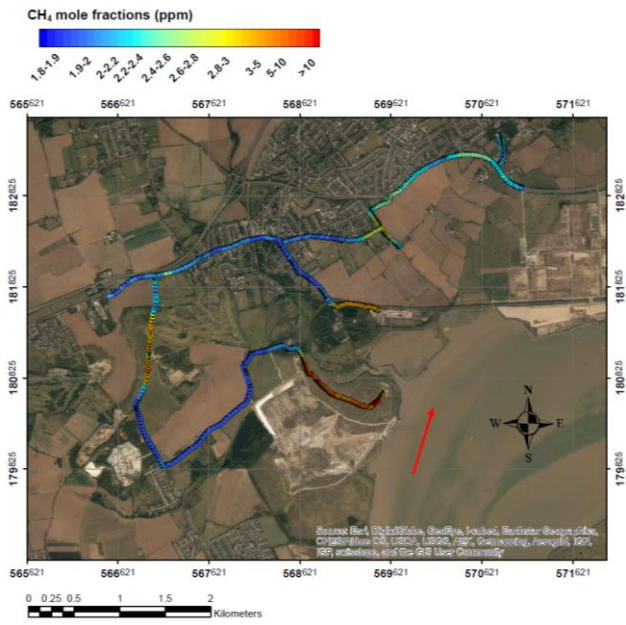
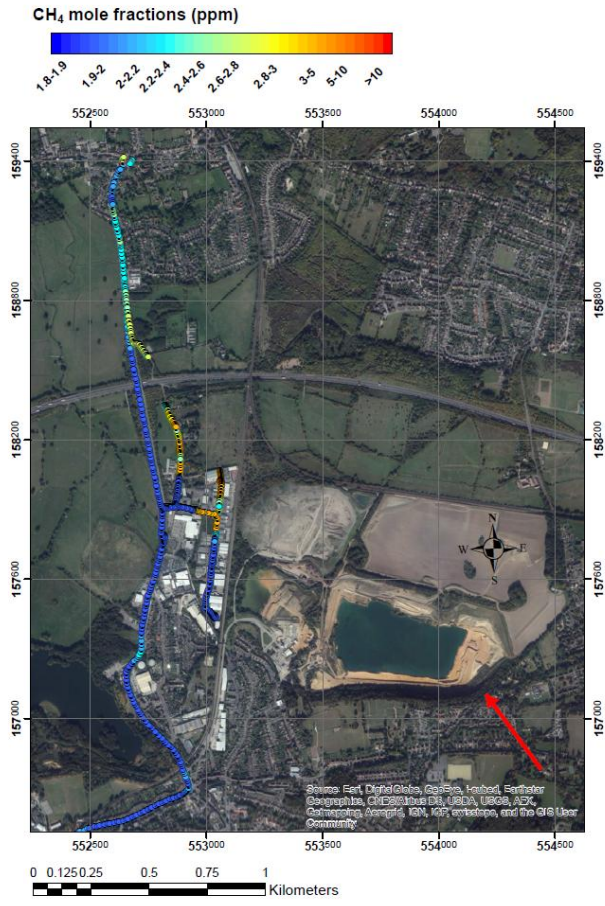


Figure 4



553

(a)



(b)

**Figure 5**

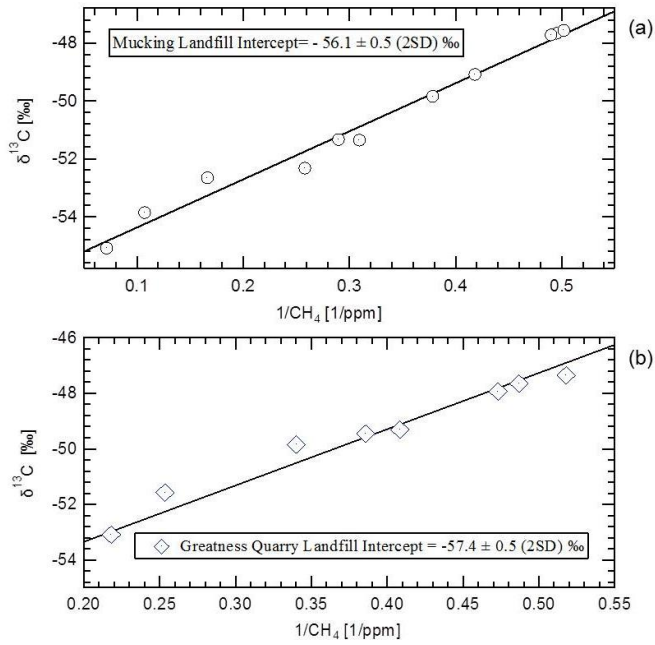


**Figure 6**





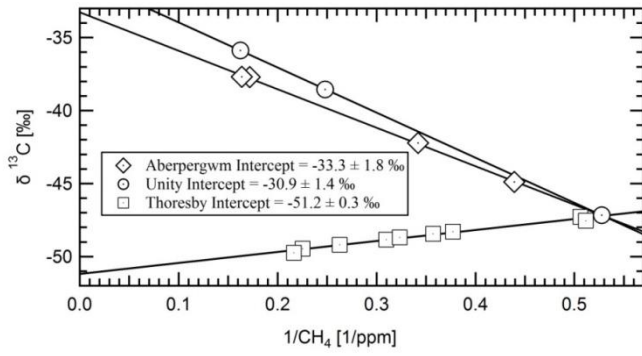


Figure 8

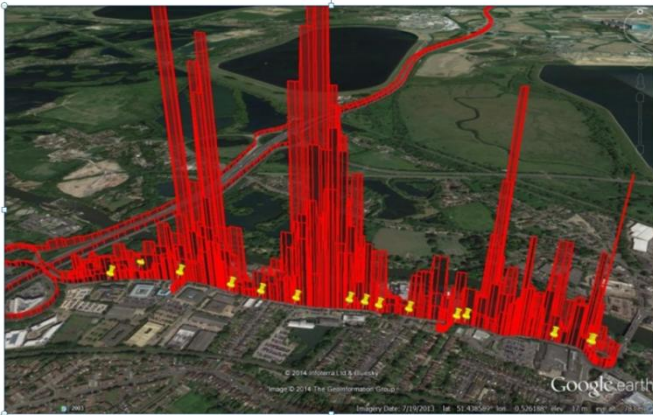


Figure 9

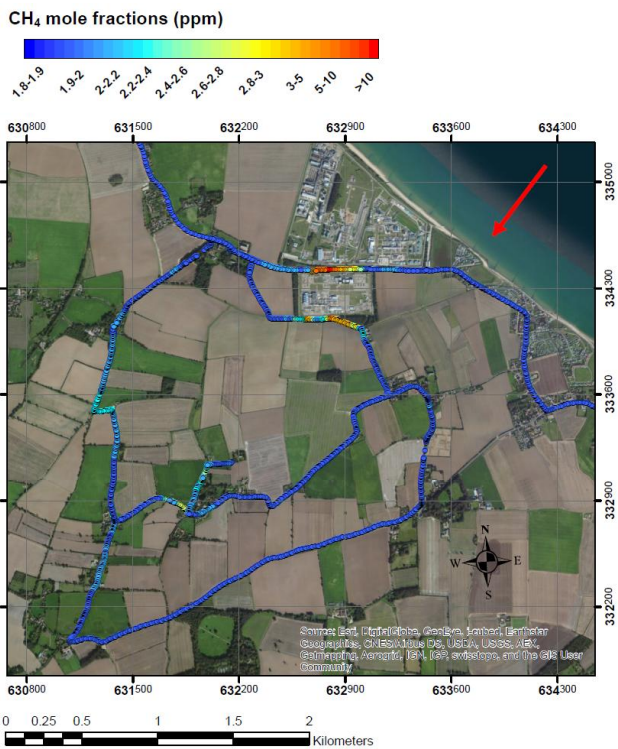
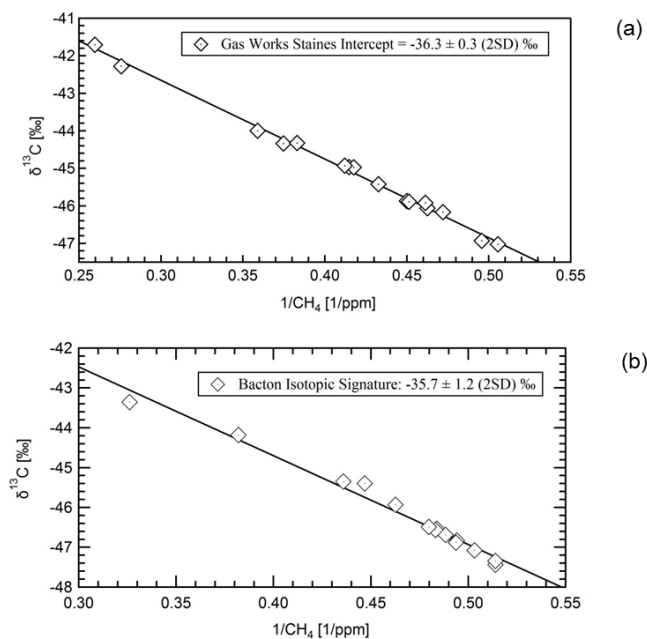


Figure 10



**Figure 11**

<i>Landfill</i>	<i>Current Status</i>	<i>Sampling Date</i>	<i>Number of samples collected</i>	$\delta^{13}\text{C}$ Signature (‰)
Albury	Active	Oct-13	4	$-59.7 \pm 1.1$
Bletchley	Active	Mar-13	26	$-58.8 \pm 0.5$
Calvert	Active	Mar-13	28	$-58.5 \pm 0.6$
Colnbrook	Closed (2012)	Jul-13	6	$-60.2 \pm 1.4$
Greatness Quarry	Active	Oct-13	8	$-57.4 \pm 0.5$
Mucking	Closed (2011)	Oct-13	11	$-56.1 \pm 0.5$
Redhill	Active	Oct-13	5	$-59.6 \pm 0.7$
Roxwell	Active	Oct-13	5	$-55.2 \pm 0.6$
Wapsey's Wood	Active	Jul-13	5	$-57.6 \pm 0.7$
		Apr-14	6	$-57.3 \pm 1.6$

554

**Table 1**

<i>Colliery</i>	<i>Current Status</i>	<i>Sampling Date</i>	<i>Number of samples collected</i>	$\delta^{13}\text{C}$ signature (‰)
Thoresby	Active	11/2013	9	$-51.2 \pm 0.3$
Aberpergwm	Closed (2012)	10/2013	4	$-33.3 \pm 1.8$
Unity	Closed (2008)	10/2013	3	$-30.9 \pm 1.4$

555

**Table 2**

<i>Gas Installation</i>	<i>Current Status</i>	<i>Sampling Date</i>	<i>Number of samples collected</i>	$\delta^{13}\text{C}$ signature (‰)
Staines	Closed (2014)	04/2014	16	$-36.3 \pm 0.3$
Bacton	Active	04/2014	14	$-35.7 \pm 1.2$

556

**Table 3**

## \*Highlights (for review)

- CH<sub>4</sub> source plumes were located by a mobile Picarro analyser
- CH<sub>4</sub> plumes from landfill sites, coal mines and gas leaks were sampled
- High precision isotopic analysis of air samples collected was carried out
- CH<sub>4</sub> isotopic signatures were allocated to CH<sub>4</sub> sources in UK
- The method provides an independent constraint to determine CH<sub>4</sub> sources contribution